

Many-body mobility edges in a one-dimensional model of interacting fermions

Sabyasachi Nag and Arti Garg

Condensed Matter Physics Division, Saha Institute of Nuclear Physics, 1/AF Bidhannagar, Kolkata 700 064, India

We analyze many body localization (MBL) in an interacting one-dimensional system with a deterministic aperiodic potential. Below the threshold value of the potential $h < h_c$, the non-interacting system has single particle mobility edges at $\pm E_c$ while for $h > h_c$ all the single particle states are localized. We demonstrate that even in the presence of single particle mobility edges, the interacting system can have MBL. Our numerical calculation of participation ratio in the Fock space and Shannon entropy shows that both for $h < h_c$ (quarter filled) and $h > h_c$ ($h \sim h_c$ and half filled), many body states in the middle of the spectrum are delocalized while the low energy states with $E < E_1$ and the high energy states with $E > E_2$ are localized. Variance of entanglement entropy (EE) also shows divergence at $E_{1,2}$ indicating a transition from MBL to delocalized regime. We also studied eigenstate thermalisation hypothesis (ETH) and found that the low energy many body states, which show area law scaling for EE do not obey ETH. The crossings from volume to area law scaling for EE and from thermal to non-thermal behaviour occurs deep inside the localised regime. For $h \gg h_c$, all the many body states remain localized for weak to intermediate strength of interaction and the system shows infinite temperature MBL phase.

PACS numbers: 72.15.Rn, 05.30.Fk, 05.30.Rt

INTRODUCTION

Interplay of disorder and interactions in quantum systems is a topic of great interest in condensed matter physics. According to the seminal work by Anderson, in a non-interacting disordered system quantum-interference among impurity scattered paths might result in a diffusion-less situation [1] due to localization. In one and two dimensions, any small amount of randomness is sufficient to localize all the single particle states while in three dimensions there occurs a single particle mobility edge leading to a metal-Anderson Insulator transition as a function of the disorder strength [2]. The question of immense interest, that has remained unanswered for decades after Anderson's work, is what happens to Anderson localization when both disorder and interactions are present in a system. Recently Basko et. al. [4] based on their perturbative treatment of interactions have established that Anderson localization can survive interactions and disordered many body eigenstates can localize resulting in a many body localized (MBL) phase, provided that interactions are sufficiently weak while strong interactions can destroy localization, resulting in a MBL transition. Followed up by this work, MBL transition has also been established non perturbatively in lattice models with finite energy density where it can extend all the way up to infinite temperatures [5, 6]. Also many works have indicated the existence of a many-body mobility edge (ME) at finite energy density in the spectrum [7–12] consistent with the fact that conductivity remains zero even at finite temperature in a MBL system [4].

The MBL phase and the MBL transition are unique for several reasons and challenge the basic foundations of quantum statistical physics [13, 14]. A hallmark of

MBL is its non-ergodicity. In the MBL phase the system explores only an exponentially small fraction of the configuration space and local observables do not thermalize leading to violation of eigenstate thermalisation hypothesis (ETH) [15–17]. MBL phase has been shown to have similarity with integrable systems [18, 19] with an extensive number of local integrals of motion [20, 21].

Recently a lot of progress has been made in the field based on numerical analysis of interacting one dimensional models of spin-less fermions or spins with completely random disorder [22–24] as well as models where there is no randomness but have a quasi-periodic potential [9, 25, 26]. An example of such model is Aubry-Andre (AA) model [27] which has a quasi-periodic potential and even in 1-d it shows a localization to delocalization transition. Interacting version of this model has been shown to have a MBL to delocalisation transition [25].

In this work we consider a deterministic aperiodic model [29] which, in the non-interacting limit, has been shown to have a tunable single particle mobility edge at $\pm E_c$ for the strength of potential $h < h_c$ while all the single particle states are localized for $h > h_c$ [30]. This model was studied recently [26] but to the best of our knowledge energy resolved analysis necessary to answer the question related to the existence of a many body ME was not done. We analyse the effect of interactions on this model for $h < h_c$ as well as for $h > h_c$ and ask the question is there a many body mobility edge in this system.

Main findings of our work based on exact diagonalisation, presented in the phase diagram of Fig. 1, are following: (1) For $h < h_c$ at half-filling, such that Fermi energy E_f lies inside the extended band, that is, $-E_c < E_f < E_c$, then in the presence of interactions this

system remains delocalized and does not show MBL. (2) But for $h < h_c$ with system less than half-filled such that in the non interacting system $E_f < -E_c$, then even in the presence of interactions, many body states with energy density $E < E_1$ and $E > E_2$ of the spectrum are localized while the intermediate energy $E_1 < E < E_2$ states are delocalized. (3) For $h > h_c$ where all single particle states are localized, interactions delocalize many body states in the middle of the spectrum for h close to h_c while for $h \gg h_c$, all the many body states remain localized for weak to intermediate strength of interactions resulting in an infinite temperature MBL phase. (4) The characteristic energy scales E_1 and E_2 are obtained from analysis of normalized participation ratio (NPR) in the Fock space and Shannon entropy. (5) These are also consistent with the transition points at which variance of entanglement entropy (EE) diverges in the thermodynamic limit. (6) Though crossover from volume to area law scaling of EE gives transition points \tilde{E}_1 and \tilde{E}_2 little off from $E_{1,2}$. For $E < \tilde{E}_1$ and $E > \tilde{E}_2$, where EE shows area scaling law, ETH is not obeyed while the intermediate energy region $\tilde{E}_1 < E < \tilde{E}_2$ is thermal and shows volume law scaling of EE.

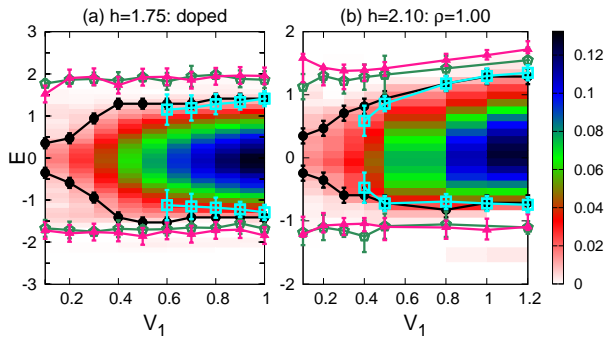


FIG. 1: Phase diagram for model in Eq.2 in E (the energy density) and V_1 plane. Left panel shows the phase diagram for $h = 1.75$ quarter filled case while the right panel shows the phase diagram for half filled $h = 2.1$ case. We have shown the value of $\eta(E)$ in the thermodynamic limit as a function of V_1 . The curves joining the full dots represent the mobility edges $E_{1,2}$ obtained from the scaling of NPR and Shannon entropy, while the curves joining diamonds and triangles represent the mobility edges $E_{1,2}$ obtained from the energy resolved entanglement entropy and the ETH respectively. For the many body states below E_1 and above E_2 , fraction of states contributing in the Fock space vanishes in the thermodynamic limit. States below \tilde{E}_1 and above \tilde{E}_2 show area-law for Renyi entropy and do not obey ETH while the states in the middle of the spectrum $\tilde{E}_1 < E < \tilde{E}_2$ show volume law for Renyi entropy and also obey ETH.

MODEL

The model we study is a generalized Aubry-Andre (AA) model of the form $H = H_0 + H_{in}$ with:

$$H_0 = -t \sum_i [c_i^\dagger c_{i+1} + h.c.] + \sum_i h_i n(i) \quad (1)$$

$$H_{in} = V_1 \sum_i n(i)n(i+1) \quad (2)$$

Here t is the nearest neighbour hopping amplitude for spin-less fermions on a one dimensional chain, h_i is the on site potential of quasi periodic form $h_i = h \cos(2\pi\alpha i^n + \phi)$ where α is an irrational number and ϕ is an offset. V_1 is the strength of repulsion between nearest neighbour fermions. Note that $n = 1$ for $V_1 = 0$ corresponds to AA model which has all single particle states localized for $h < 2t$ and all the states are delocalised for $h > 2t$. But for $n < 1$ and for $V_1 = 0$, Hamiltonian in Eq. 2 is known to have a single particle mobility edge at $E_c = \pm[2t - h]$ [30]. For $h > 2t$, all single particle states are localized. We think that this is an interesting model to study MBL because by tuning h one can tune the fraction of delocalised to localized single particle states in the non-interacting system and analyze how localized and delocalised states interact with each other. We study this model for $h < 2t$ as well as for $h > 2t$ using exact diagonalisation for various parameter values and analyze how localized and extended (or weakly localized) single particle states interact resulting in many-body mobility edge.

RESULTS

The results described in the following sections are obtained by solving the model in Eq. 2 using exact diagonalization on finite size chains with open boundary conditions. Everywhere we choose $\alpha = \frac{\sqrt{5}-1}{2}$ and $n = 0.5$. We present results for $h = 1.75t$ for which single particle spectrum has a mobility edge as well as for $h = 2.1t$ and $6t$ for which all single particle states are localized. For $h = 1.75t$, we present results for the half filled case, i.e. with particle density $\rho = 1$ as well as for $\rho = 0.25$. The phase diagram shown in Fig. 1 has been obtained on the basis of analysis of various quantities namely, energy spacing statistics, normalized participation ratio, Shannon entropy, Renyi entropy and ETH. Below we describe our results for each of these one by one.

Energy level spacing statistics

A convenient measure to differentiate between the localized and extended states is based on study of spectral statistics using tools from random matrix theory [32].

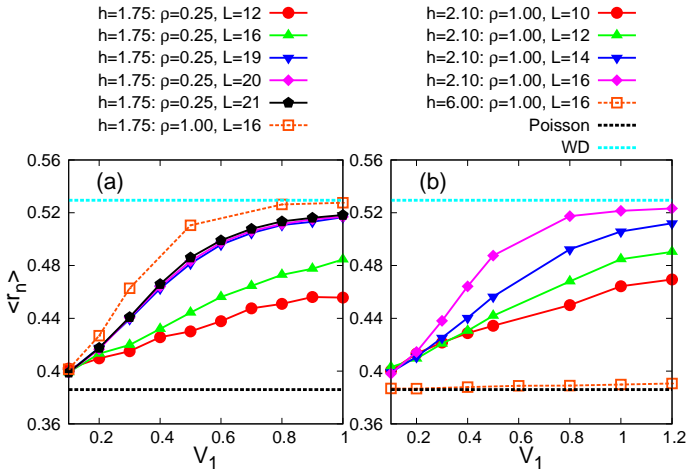


FIG. 2: Plot of $\langle r \rangle$ averaged over the entire spectrum vs V_1 for various system sizes. Left panel shows the results for $h = 1.75t < h_c$. Full curves show data for doped case with $\rho = 0.25$ for various L values. $\langle r \rangle$ increases with L as well as with V_1 approaching the WD value for $V_1 \sim t$. Note that for a given L , $\langle r \rangle$ for the half filled case is much larger than the corresponding values for $\rho = 0.25$ case and is closer to the WD value. The right panel shows $\langle r \rangle$ data for $h > h_c$ case. For $h = 2.1t$ for most of the values of V_1 in weak to intermediate regime, $\langle r \rangle$ is much below the value for WD distribution. Only for $V_1 \sim t$ $\langle r \rangle$ starts approaching WD value. On the other hand for $h = 6t \gg h_c$, $\langle r \rangle \sim 0.386$ for all the values of V_1 studied indicating that all the many body states are localized even in the presence of interaction.

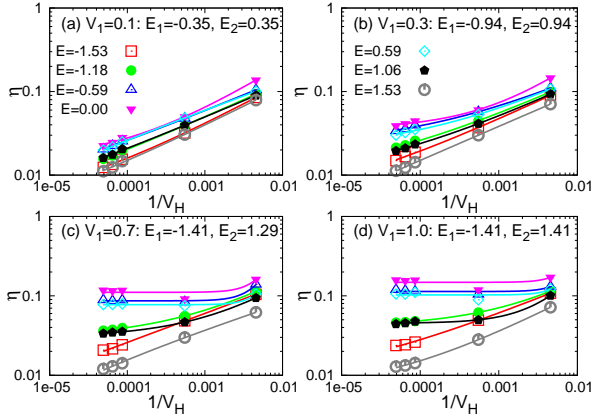


FIG. 3: $\eta(E)$ vs $1/V_H$ for various values of E . The top panel shows result for $h = 1.75t$ doped case. Here for $V_1 = 0.1t$, $\eta(E) \sim b * V_H^{-c}$ for all values of E except for a few states with $E \sim 0$ where $\eta(E) \sim a + b * V_H^{-c}$. On increasing V_1 more many body states get delocalized as indicated in panel (b). Bin size used is $dE = 0.08t$. The bottom panel shows results for $h = 2.1t$ half filled case (bin size used is $0.04t$).

The distribution of energy level spacings is expected to follow Poisson statistics for many body localized phase while it follows Wigner-Dyson statistics for the ergodic phase. This is based on the intuition that in a localized

phase, states which are close in energy live very far in the configuration space to be mixed by the kinetic energy and therefore the level repulsion is suppressed in the localized phase resulting in Poisson statistics for level spacings. On the other hand in an ergodic phase, disorder lifts degeneracies resulting in strong level repulsion leading to Wigner-Dyson statistics. Following [5], we calculate the ratio of successive gaps in energy levels $r_n = \frac{\min(\delta_n, \delta_{n+1})}{\max(\delta_n, \delta_{n+1})}$ with $\delta_n = E_{n+1} - E_n$ at a given eigen energy E_n of the Hamiltonian in Eq. 2 to discriminate between the two phases. For a Poissonian distribution, the disorder averaged value of r is $2\ln 2 - 1 \approx 0.386$; while for the Wigner surmise of Gaussian orthogonal ensemble (GOE) mean value of $r \approx 0.5295$.

Fig. 2 shows the plot of average r vs the interaction strength V_1 for various system sizes. This data is obtained from r_n averaged over the entire energy spectrum for a given configuration of quasi-periodic potential and then averaged over 50-100 independent configurations obtained by varying ϕ . For $h = 6t$, $\langle r \rangle$ is close to Poisson value for all values of interactions indicating the presence of a MBL phase. But both, for $h = 1.75t$ with particle density 0.25 and $h = 2.1t$ with half-filling, $\langle r \rangle$ is close to the Poisson value for very small values of V_1 . $\langle r \rangle$ increases with system size L and starts approaching the Wigner-Dyson value for large V_1 values. But for most of the range of interactions, $\langle r \rangle$ is somewhere in between the two values, indicating that different parts of the energy spectrum might have different behaviour such that the average is neither close to the Poisson limit nor to the WD limit. Note that for $h = 1.75t$ at half filling, $\langle r \rangle$ is larger than its value for the quarter filled case and approaches wigner-dyson value for weaker strength of V_1 indicating that many body states for $h < h_c$ half-filled system are more extended than the states for the quarter filled case.

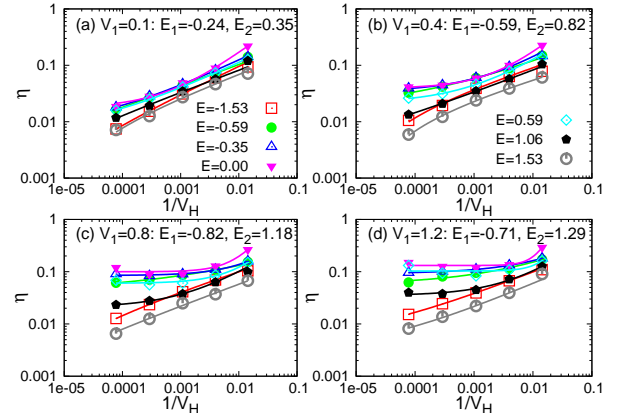


FIG. 4: Same as in Fig. 3 for $h = 2.1t$ half filled case. Bin size used here is $dE = 0.04t$.

Normalized Participation ratio in Fock space(NPR)

To decide whether a many-body state is localized or not, we calculate the NPR which is defined as

$$\eta(E) = \frac{1}{\langle \sum_{i,n} |\Psi_n(i)|^4 \delta(E - E_n) \rangle_C V_H} \quad (3)$$

where $\Psi_n(i)$ is an eigenfunction (normalized) with eigenvalue E_n of the Hamiltonian in Eq. 2, V_H is the volume of the Fock space, and $\langle \rangle_C$ indicates the configuration averaging. In our numerical calculation of $\eta(E)$, we replace the delta function by a box distribution of finite width dE around energy density $E = E_n/N_p$ where N_p is the number of particles in the system. $\eta(E)$ represents the fraction of configuration space participating in a many-body state of energy E .

Fig. 3 shows scaling of $\eta(E)$ w.r.t $1/V_H$ for $h = 1.75t$ and $\rho = 0.25$. For very low and high energy states, $\eta(E)$ decreases as the system size increases going to zero in the thermodynamic limit ($\eta(E) \sim bV_H^{-c}$) indicating localized nature of these many body states. For states in the middle of the band $\eta(E) \sim a + b(1/V_H)^c$ with finite value a in the thermodynamic limit indicating the ergodic nature of these states. Extrapolated values of $\eta(E)$ in the thermodynamic limit are shown in the density plot of Fig. 1. From the extrapolated values, we obtained two transitions from MBL states to delocalized states at energy densities E_1 and E_2 (shown in black curves in Fig. 1) such that states with $E < E_1$ and $E > E_2$ are localized while states with $E_1 < E < E_2$ are extended indicating the presence of two MEs in the many body spectrum. For $h = 2.1t$, at half filling, we get a similar picture from the analysis of NPR, shown in Fig. 4. Here, since all single particle states are localized for $V_1 = 0$, all the many body states are localized for $V_1 = 0$. But for non zero V_1 , states in the middle of the many body spectrum gets delocalized. This happens because $h = 2.1t$ is very close to h_c and some of the single particle states are very weakly localized.

Shannon Entropy

We also calculate Shannon entropy for every eigenstate $S(E_n) = -\sum_{i=1}^{V_H} |\Psi_n(i)|^2 \ln |\Psi_n(i)|^2$. Clearly for a many body state which gets contribution from all the basis states in the Fock space (and is normalized) $S(E_n) \sim \ln(V_H)$ and thus $f(E) = \exp(S(E_n))/V_H \sim 1$ while for a localized state which gets significant contribution only from some of the basis states, say N_l , in the Fock space, then $f(E) = \exp(S(E_n))/V_H \sim N_l/V_H$ vanishing to zero in the thermodynamic limit. Fig. 5 shows the plot for $f(E)$ vs E for various system sizes for $h = 1.75t$ doped case. Though for very small V_1 , $f(E)$ decreases with increasing system sizes for all values of E ,

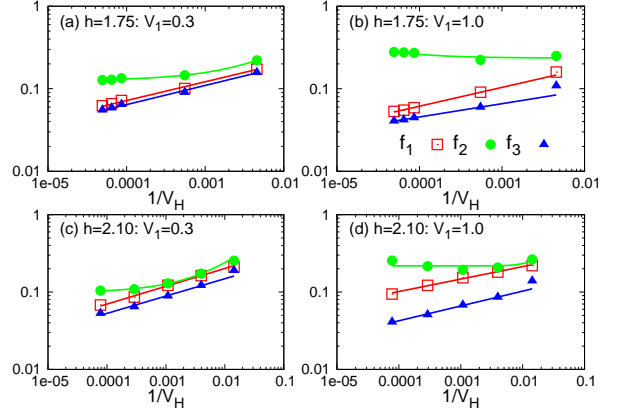


FIG. 5: $f(E) = \exp(S(E_n))/V_H$ in three regions of many body spectrum obtained by NPR analysis. The top panel shows scaling of f_1 which is $f(E)$ averaged over all $E < E_1$, f_3 which is $f(E)$ averaged over $E > E_2$ and f_2 which is $f(E)$ averaged for $E_1 < E < E_2$ for $h = 1.75t$ less than half-filled case. Both for $V_1 = 0.1t$ and $V_1 = 0.8t$, f_1 and f_2 vanish in the thermodynamic limit while f_2 stays finite indicating the delocalised nature of states in the middle region of the spectrum. The bottom panels shows scaling of $f_{1,2,3}$ for $h = 2.1t$ half filled case.

the extrapolated value of f in the thermodynamic limit is not zero for all E values. The bottom panel shows scaling of $f_{1,2,3}$ which are obtained by averaging $f(E)$ over three regions of the spectrum, namely, $E < E_1$, $E_1 < E < E_2$ and $E > E_2$. In close analogy to the NPR, f_2 is finite in the thermodynamic limit while f_1 and f_3 vanish indicating again the crossover from MBL to delocalised nature of states across the spectrum. A similar picture emerges for $h = 2.1t$ half filled case where also from the analysis of Shannon entropy we concluded that there is a many-body mobility edge in this model. Details of this are presented in Appendix A.

Comparison of $h < h_c$ less than half-filled and half-filled case

Before we present our analysis of the entanglement entropy, we would like to compare the $h < h_c$ half filled case and the quarter filled case based on our current analysis of NPR and Shannon entropy. So far we presented effect of interaction on system where in the non-interacting case Fermi energy lies below the single particle mobility edge E_c . Thus not only the states below the Fermi energy are localized, but many of states above it are localized too. In such a scenario, one of course expects the many body ground state and some of the excited states to show localization which already hints towards the presence of a many-body mobility edge in this system. Our numerical study, presented above, demonstrated that even in the presence of interactions, of weak to intermediate strength, there is a mobility edge $E_{1,2}$ which separates

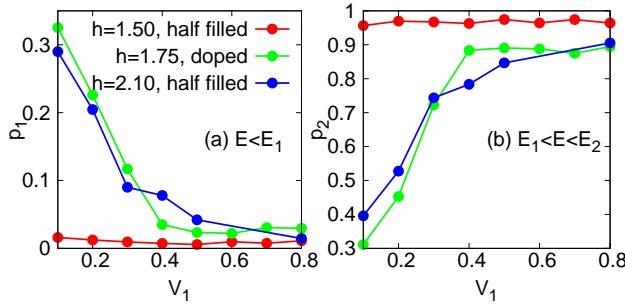


FIG. 6: Fraction of states vs V_1 in the localized and delocalised sector of the spectrum based on NPR analysis. Left panel shows the fraction for the localized sector on the low energy density side for $h < h_c$ as well as for $h > h_c$. Note that for $h < h_c$ ($h = 1.75t$, $\rho = 0.25$), there is a finite fraction of many body states which show localization while for half filled $h < h_c$ case (e.g. $h = 1.5t$, $\rho = 1$), fraction of states in the localized sector of the many body spectrum is vanishingly small. For $h > h_c$ even at $\rho = 1$, there is a finite fraction of states in the localized sector. Right panel shows the results for fraction in the middle part of the spectrum which is delocalized.

the many body states (below E_1 and above E_2) showing MBL from the states which are delocalised. As the interaction strength increases more many body states in the middle of the spectrum get delocalised. Now consider the half filled case for $h < h_c$. Though in the non-interacting case there are mobility edges $\pm E_c$, but the Fermi energy is now in the middle of delocalised band. Though some of states below Fermi energy are localized, but states near the Fermi energy are all extended making this system metallic. In this case, if one does finite size analysis of NPR and Shannon entropy for the interacting system, one again finds $\eta(E)$ or $f(E)$ vanishing in the thermodynamic limit for $E < E_1$ and $E > E_2$ just like the quarter filled case, details of which are given in Appendix B. We calculate the fraction of states below E_1 , above E_2 and in the intermediate energy regime for further analysis. For every configuration, we count number of energy states for a given L below E_1 and divide it by the total number of states V_H . We further average it over independent configurations and get p_1 . Similarly we obtain p_2 and p_3 which satisfy for any value of parameter set $\sum_i p_i = 1$. Fig. 6 shows the fraction of states for $h = 1.75t < h_c$ as a function of the interaction strength. We clearly see that p_1 for the half filled case is vanishingly small and is much smaller than the value for the quarter filled case supporting our physical picture that there is no MBL for $h < h_c$ half filled case while there is a many body mobility edge for $h < h_c$ quarter filled case. We have also shown for comparison the fraction of states for $h = 2.1t > h_c$ case at half filled where the fraction of states in the localized regime is finite and decreases with the interaction

strength indicating a MBL to delocalization transition.

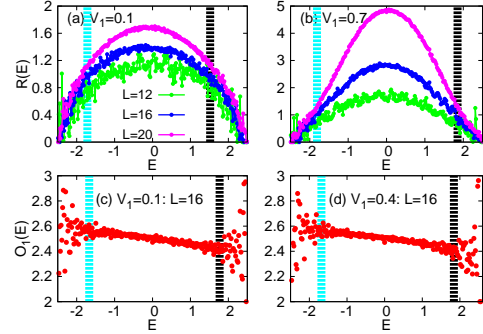


FIG. 7: Top panel shows energy resolved $R(E)$ vs E for $h = 1.75t$ and $\rho = 0.25$ for various values of L . There is a characteristic energy \tilde{E}_1 below which $R(E)$ is same for all L values within numerical error and same holds true for $E > \tilde{E}_2$. But for the intermediate states $\tilde{E}_1 < E < \tilde{E}_2$, $R(E)$ shows volume scaling law and increases with L indicating its ergodic nature. The ergodic regime increases with increase in V_1 as shown in the right panel for $V_1 = 0.7t$. The bottom panel shows expectation value of \hat{O} , which is the sum of number operators over subsystem A, vs E . Again below the characteristic energy which is close to \tilde{E}_1 , $O(E)$ shows large fluctuations in its value for near by eigenstates and same holds true for $E > \tilde{E}_2$. But for the intermediate regime $\tilde{E}_1 < E < \tilde{E}_2$, fluctuations of $O(E)$ among nearby energy states is small indicating its thermal nature. This data is obtained by binning over a bin in energy of size $dE = 0.02t$.

Entanglement Entropy

Entanglement entropy (EE) characterizes how information spreads from one part of the system to another and is a useful tool to distinguish between the ergodic and many-body localized phases. We divide the lattice into two subsystems A and B of sites $L/2$ and calculate the energy resolved Renyi entropy $R(E_n) = -\log[Tr_A \rho_A(E_n)^2]$ where ρ_A is the reduced density matrix obtained by integrating the total density matrix $\rho_{total}(E_n) = |\Psi_n\rangle\langle\Psi_n|$ over the degree of freedom of subsystem B. EE is expected to obey the volume law of scaling $R \sim L^d$ in the ergodic phase while the EE is suppressed for the MBL phase showing an area law scaling $R \sim L^{d-1}$ [9]. Here d is the physical dimension of the system.

Fig. 7 shows $R(E)$ which is obtained from $R(E_n)$ by binning over an energy bin dE around energy E and averaging over 50-100 configurations. For $E < \tilde{E}_1$, $R(E)$ is same for various system sizes indicating that the many body states in this energy regime are localized with $R(E)$ obeying area law ($R(E) \sim L^0$). Same is true for many body states at the top of the spectrum with $E > \tilde{E}_2$, while for many-body states in the middle of the spectrum $\tilde{E}_1 < E < \tilde{E}_2$, $R(E) \sim L$ indicating their delocalised nature. As the strength of the interaction increases, the re-

gion of delocalised states increases. We would like to emphasize that this picture is qualitatively consistent with what we obtained from the analysis of NPR and Shannon entropy though values of $\tilde{E}_{1,2}$ are little off from $E_{1,2}$ obtained earlier, which can be seen clearly in Fig. 1. In Fig. 1, curves passing through full circles represent $E_{1,2}$ while curves passing through hexagons represent $\tilde{E}_{1,2}$. This indicates that there is a regime where many body states are localized in Fock space but still EE increases with L .

We also calculated EE for $h = 2.1t$ half filled case as well and saw clear indications of ME, details of which are given in Fig. 8.

Eigenstate Thermalisation Hypothesis

In this section we check for the ETH in various parameter regimes by calculating expectation value of the number operator on subsystem A which has $L/2$ sites w.r.t various eigenstates. We define $\hat{O} = \sum_{i=1}^{L/2} \hat{n}_i$ where \hat{n}_i is the number operator for spinless fermions at site i . For every eigenstate, we calculate the expectation value $\langle O \rangle_n = \langle \Psi_n | \hat{O} | \Psi_n \rangle$ and from their obtained $O(E)$ which is obtained by averaging $O(E_n)$ over all E_n values which belong to the bin $E \pm dE$. This is further averaged over many independent configurations. For an ergodic phase, $O(E)$ does not have large fluctuations for nearby eigenstates.

Fig. 8 shows $O(E)$ as a function of E for $h = 1.75$ quarter filled system. We observe that for states with $E < \tilde{E}_1$ and $E > \tilde{E}_2$, many body system is not thermal showing violation of ETH while for $\tilde{E}_1 < E < \tilde{E}_2$, system is ergodic and obeys ETH. Further as it is clear from Fig 7, that $\tilde{E}_{1,2} \sim \tilde{E}_{1,2}$ within numerical error indicating that the transition from non-thermal to thermal phase occurs at the same energy at which the EE shows transition from area to volume law of scaling. This is clearly shown in the Fig. 1 where curves joining triangles show $\tilde{E}_{1,2}$. We did similar analysis for $h = 2.1t$ half filled case as well and the result is shown in Fig. 8.

Variance of EE

We also calculated the variance of EE $\delta_R(E) = \langle R(E)^2 \rangle - \langle R(E) \rangle^2$ shown in Fig. 9 for various values of V_1 . In the thermodynamic limit δ_R should be zero deep inside the localized and delocalised phases but at the transition point it diverges due to contribution from both the extended and the localized states [7] which is reflected as a peak in finite size calculations. Our data shows two clear peaks in $\delta_R(E)$ vs E curve for a given V_1 indicating two transition points which are very close to $E_{1,2}$ obtained from NPR analysis as shown in Fig. 1

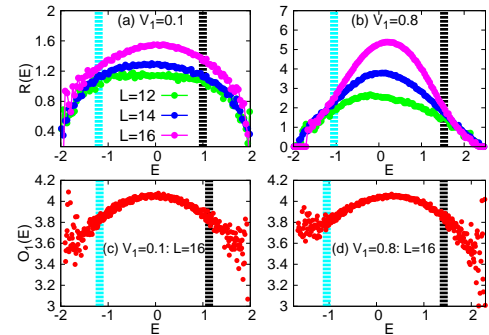


FIG. 8: Same as in Fig. 7 for $h = 2.1t$ and $\rho = 1$. This data is obtained by binning over a bin in energy of size $dE = 0.01t$.

where blue curves represent peak positions in $\delta_R(E)$ vs E curve. Note that for small values of V_1 the two peaks in $\delta_R(E)$ vs E curve are very close to each other and it is difficult to identify the peak positions precisely.

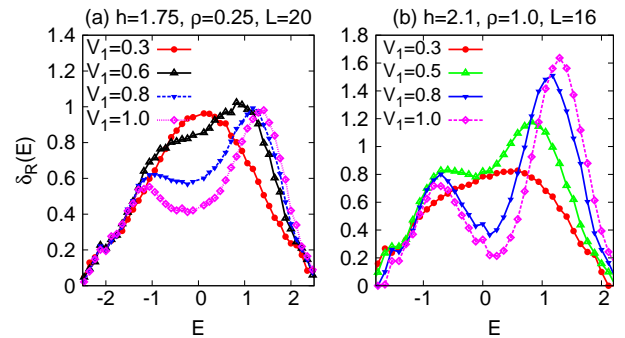


FIG. 9: Variance $\delta_R(E)$ of EE over the disorder ensemble as a function of E for various values of V_1 . $\delta_R(E)$ shows two clear peaks, indicating the localisation to delocalization transition.

Based on this numerical analysis we demonstrated that both for $h < h_c$ and $\rho = 0.25$ and for $h > h_c$ half filled case, there are many-body MEs $E_{1,2}$ which are determined from NPR, Shannon entropy and variance of EE. Further a transition from non thermal phase to thermal phase, which obeys ETH and the volume law for EE, occurs inside the localized regime. For $h \gg h_c$, this model shows infinite temperature MBL phase where all many body states are localized which was clearly indicated from energy level statistics which obeys Poisson statistics for weak to intermediate strength of V_1 .

CONCLUSIONS

In summary we have analysed MBL in an interacting 1-d model of spin-less fermions in the presence of an aperiodic potential. The non-interacting system has mobility edges at $\pm E_c$ for $h < h_c$ while all the single particle states are localized for $h > h_c$. We demonstrated that if $E_f < -E_c$, the interacting system undergoes two

many body localisation to delocalization transitions as a function of energy density indicating the presence of two mobility edges in the many body spectrum. MBL states live on the low and very high energy part of the spectrum while the middle of the spectrum has delocalized states. If in the noninteracting case for $h < h_c$, E_f lies inside the extended band such that the ground state is extended, then in the interacting system all the many body states remain delocalized. For $h > h_c$ but close to h_c , when all single particle states are localized, interactions lead to delocalization of states in the middle of the many body spectrum. Only for $h \gg h_c$, interacting system shows infinite temperature MBL phase. Further we demonstrated that the mobility edges obtained from NPR in Fock space is consistent with those obtained from variance of EE. Though transition from area to volume law scaling of EE are accompanied by non-thermal to thermal transition based on the analysis of ETH, these transition points lie inside the localized regime.

APPENDIX A

In this Appendix, we give details of the extrapolated values of the Shannon entropy for $h = 1.75t$ and $\rho = 0.25$.

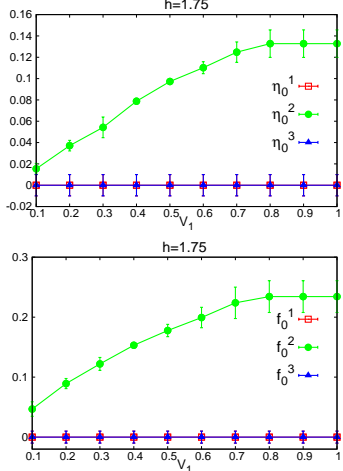


FIG. 10: Extrapolated value of energy resolved NPR $\eta(E)$ vs V_1 for $h = 1.75t$ and $\rho = 0.25$. Here η_1 is obtained by doing averaging of extrapolated $\eta_0(E)$ over $E < E_1$, η_2 is obtained by averaging $\eta_0(E)$ over $E_1 < E < E_2$ and η_3 is $\eta_0(E)$ averaged over $E > E_2$ regime. Right panel shows extrapolated values of $f(E)$ obtained from Shannon entropy in three regimes.

APPENDIX B

In this appendix, we present details of results for $h < h_c = 1.5t$ half filled case.

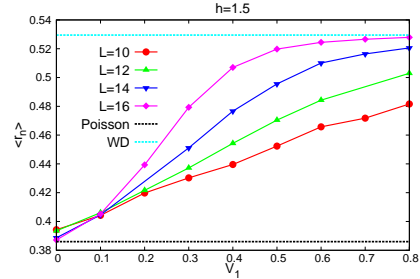


FIG. 11: Average $\langle r \rangle$, averaged over the entire spectrum for $h = 1.5t$ half filled case, vs V_1 for various values of L .

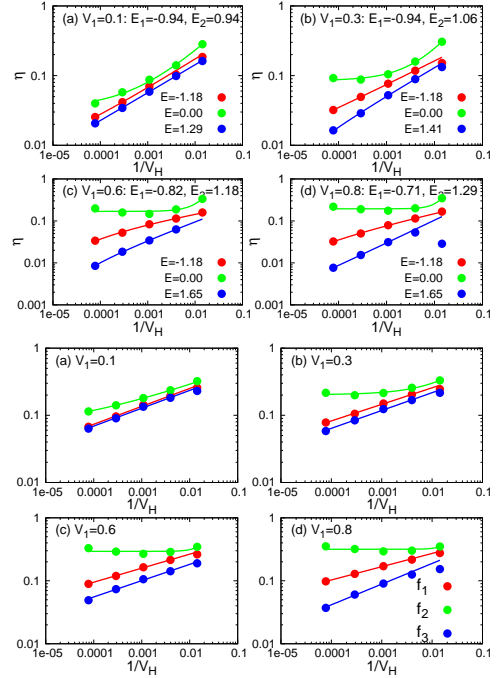


FIG. 12: Left panel shows scaling of $\eta(E)$ w.r.t. $1/V_H$ for various E states at different values of V_1 . Right panel shows the scaling for $f(E)$ obtained by averaging $\exp(S(E))/V_H$ over $E < E_1$ (that gives f_1), over region two $E_1 < E < E_2$ (that gives f_2) and over third region $E > E_2$ that gives f_3 .

- [1] P. W. Anderson, Phys. Rev. **109**, 1492 (1958).
- [2] E. Abrahams, P. W. Anderson, D. C. Licciardello, and T. V. Ramakrishnan, Phys. Rev. Lett. **42**, 673 (1979).
- [3] P. A. Lee and T. V. Ramakrishnan, Rev. Mod. Phys. **57**, 287 (1985).
- [4] D. M. Basko, I. L. Aleiner, and B. L. Altshuler, Ann. Phys. (Amsterdam), **321**, 1126 (2006).
- [5] V. Oganesyan and D. A. Huse, Phys. Rev. B **75**, 155111 (2007).

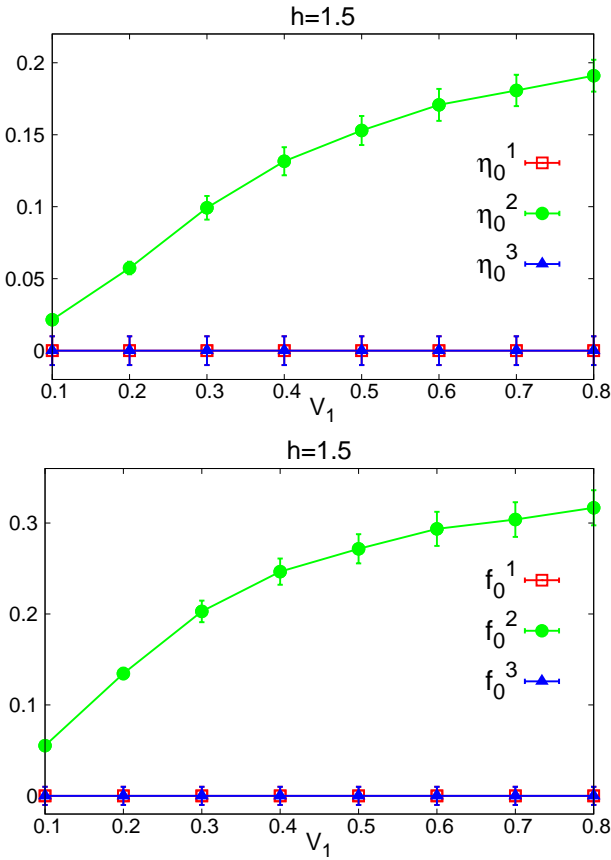


FIG. 13: Extrapolated value of energy resolved NPR $\eta(E)$ vs V_1 for $h = 1.5t$ half-filled case. Here η_1 is obtained by doing averaging of extrapolated $\eta_0(E)$ over $E < E_1$, η_2 is obtained by averaging $\eta_0(E)$ over $E_1 < E < E_2$ and η_3 is $\eta_0(E)$ averaged over $E > E_2$ regime. Right panel shows extrapolated values of $f(E)$ obtained from Shannon entropy in three regimes.

- [6] A. Pal and D. A. Huse, Phys. Rev. B **82**, 174411 (2010).
- [7] J. A. Kjall, H. H. Bardarson, and F. Pollmann, Phys. Rev. Lett. **113**, 107204 (2014).
- [8] D. J. Luitz, N. Laflorencie, F. Alet, Phys. Rev. B **91**,

- 081103(R) (2015).
- [9] X. Li, S. Ganeshan, J. H. Pixley, and S. D. Sarma, Phys. Rev. Lett. **115**, 186601 (2015).
- [10] C. R. Laumann, A. Pal, and A. Scardicchio, Phys. Rev. Lett. **113**, 200405 (2014).
- [11] I. Mondragon-Shem, A. Pal, T. L. Hughes, and C. R. Laumann, Phys. Rev. B **92**, 064203 (2015).
- [12] P. Naldesi, E. Ercolessi, and T. Roscilde, SciPost Phys. **1**, 010 (2016).
- [13] R. Nandkishore and D. A. Huse, Ann. Rev. Cond. Matt. Phys. **6**, 15 (2015).
- [14] E. Altman and R. Vosk, Ann. Rev. Cond. Matt. Phys. **6**, 383 (2015).
- [15] J. M. Deutsch, Phys. Rev. A **43**, 2046 (1991).
- [16] M. Srednicki, Phys. Rev. E **50**, 888 (1994).
- [17] M. Rigol, V. Dunjko, and M. Olshanii, Nature (London), **452**, 854 (2008).
- [18] D. A. Huse, R. Nandkishore, and V. Oganesyan, Phys. Rev. B **90**, 174202 (2014).
- [19] R. Modak, S. Mukerjee, E. A. Yuzbashyan, and B. S. Shastry, arXiv:1503.07019.
- [20] M. Serbyn, Z. Papic, and D. A. Abanin, Phys. Rev. Lett. **111**, 127201 (2013).
- [21] V. Ros, M. Mueller, and A. Scardicchio, Nucl. Phys. B **891**, 420 (2015).
- [22] S. Bera, H. Schomerus, F. H-Meisner, and J. H. Bardarson, Phys. Rev. Lett. **115**, 046603 (2015).
- [23] T. Enss, F. Andraschko, J. Sirker, arXiv:1608.05733.
- [24] V. Ros and M. Mueller, arXiv:1608.06225.
- [25] S. Iyer, V. Oganesyan, G. Refael, and D. A. Huse, Phys. Rev. B **87**, 134202 (2013).
- [26] R. Modak and S. Mukerjee, Phys. Rev. Lett. **115**, 230401 (2015).
- [27] S. Aubry and G. Andre, Ann. Isr. Phys. Soc. **3**, 18 (1980).
- [28] J. Vidal, D. Mouhanna and T. Giamarchi, Phys. Rev. Lett. **83**, 3908 (1999);
- [29] M. Griniasty and S. Fishman, Phys. Rev. Lett. **60**, 1334 (1988).
- [30] S. Das Sarma, S. He, and X. C. Xie, Phys. Rev. B **41**, 5544 (1990).
- [31] M. Schreiber, S. S. Hodgmann, P. Bordia, H. P. Lschen, M. H. Fischer, R. Vosk, E. Altman, U. Schneider, and I. Bloch, Science **349**, 842 (2015).
- [32] M. L. Mehta, *Random Matrices* (Academic, Boston, 1991).

$h=1.75: n=0.25, L=12$ 
 $h=1.75: n=0.25, L=16$ 
 $h=1.75: n=0.25, L=19$ 
 $h=1.75: n=0.25, L=20$ 
 $h=1.75: n=0.25, L=21$ 
 $h=1.75: n=1.00, L=16$ 

$h=2.10: n=1.00, L=10$ 
 $h=2.10: n=1.00, L=12$ 
 $h=2.10: n=1.00, L=14$ 
 $h=2.10: n=1.00, L=16$ 
 $h=6.00: n=1.00, L=16$ 
Poisson 
WD 

